Hindawi
Journal of Nanomaterials
Volume 2017, Article ID 2565703, 6 pages
https://doi.org/10.1155/2017/2565703

*Research Article*

# Modulation of Optical and Electrical Characteristics by Laterally Stretching DNAs on CVD-Grown Monolayers of $MoS_2$

**Guru P. Neupane, Minh Dao Tran, Hyun Kim, and Jeongyong Kim**

*Department of Energy Science, Sungkyunkwan University (SKKU), Suwon 440-746, Republic of Korea*

Correspondence should be addressed to Jeongyong Kim; j.kim@skku.edu

Received 16 November 2016; Revised 22 February 2017; Accepted 9 March 2017; Published 19 March 2017

Academic Editor: Yu-Lun Chueh



Monolayer $MoS_2$ (1L-$MoS_2$) is an ideal platform to examine and manipulate two dimensionally confined exciton complexes, which provides a large variety of modulating the optical and electrical properties of 1L-$MoS_2$. Extensive studies of external doping and hybridization exhibit the possibilities of engineering the optical and electrical performance of 1L-$MoS_2$. However, biomodifications of 1L-$MoS_2$ and the characterization and applications of such hybrid structures are rarely reported. In this paper, we present a bio-$MoS_2$ hybrid structure fabricated by laterally stretching strands of DNAs on CVD-grown 1L-$MoS_2$. We observed a strong modification of photoluminescence and Raman spectra with reduced PL intensity and red-shift of PL peak and Raman peaks, which were attributed to electron doping by the DNAs and the presence of tensile strain in 1L-$MoS_2$. Moreover, we observed a significant enhancement of electric mobility in the DNA/1L-$MoS_2$ hybrid compared to that in the pristine 1L-$MoS_2$, which may have been caused by the induced strain in 1L-$MoS_2$.

## 1. Introduction

Monolayers of transition metal dichalcogenides (1L-TMDs) are atomically thin direct band gap semiconductors [1–4], which host two dimensionally confined exciton complexes such as neutral excitons, trions, and biexcitons. These excitons system predominantly provoke the optoelectronic characteristics of 1L-TMDs, particularly 1L-$MoS_2$ [1–4]. Therefore, the manipulation of such exciton systems has been a key to modulate the optoelectronic characteristics of 1L-$MoS_2$ [5–11]. Electrostatic gating [5], surface plasmon [6, 7], chemical doping [8, 9], and strain engineering [10, 11] are promising ways to influence the population of the excitons complexes, where reversible electrostatic tunability of neutral excitons to trions has been demonstrated. When 1L-$MoS_2$ was hybridized with metallic nanoparticles, the excitation of localized surface plasmons provided the enhancement of the photoluminescence (PL) from $MoS_2$ [6, 7]. In the chemical doping process, the charge transfer between the dopant molecules and 1L-$MoS_2$ modulated the intrinsic optoelectronic characteristics [8, 9]. The enhancement or reduction of the PL intensity of 1L-$MoS_2$ depended upon the nature of doping (n-type or p-type chemicals) [8, 9, 12]. During the n-type doping process, the increase of electron density resulted in a dominance population of trions over the neutral excitons and the intrinsically faster nonradiative recombination of trions lowered the PL efficiency of n-type 1L-$MoS_2$ [9, 12]. The higher chance of exciton-exciton annihilation at higher carrier density is also responsible for reducing the PL intensity [13]. On the contrary, the p-doping of 1L-$MoS_2$ caused an increase in the spectral weight of neutral excitons and in the PL intensity [9].

Furthermore, strain engineering has been a consistent route for the modulation of the optoelectronic characteristics of 1L-$MoS_2$. Several theoretical and experimental results have demonstrated that the application of uniaxial or isotropic strains can modulate the band gap of monolayer 1L-$MoS_2$ and can even induce the phase change from the direct gap to an indirect gap and thus have a significant effect on the PL intensity of 1L-$MoS_2$ [14–17]. It has also been suggested that strain engineering of the band structure of $MoS_2$ could be useful for increasing the carrier mobility of $MoS_2$ [15, 18].

While there have been many efforts to create hybrid structures of TMDs for enhanced physical and chemical

characteristics [19–22], the hybridization of biomaterials and TMDs is relatively rare. Recently, ultra-high sensitivity field-effect transistor (FET) sensor using DNA-TMD system has been demonstrated [23], and DNA inducing doping effect on thick TMDs materials have been introduced [24, 25]. Biomolecules and TMD materials hold significant potential for the development of extremely small devices with increasingly complex functionality, which could open various applications in bioelectronics. Particularly, 1L-TMDs display the strong optical emission due to their direct band gap nature [1–4], and thus biohybridization of 1L-TMDs suggests promising optoelectronic applications. However, DNA-TMD hybrid structure using 1L-TMDs and the consequent modulation of optical properties of 1L-TMDs was not studied so far.

In this study, we present a hybrid structure of laterally stretched DNA strands on 1L-$MoS_2$. Significant modifications in PL intensity and Raman spectra of 1L-$MoS_2$ were observed, which indicated the n-doping effect and tensile strain caused by hybridization with stretched DNA strands. Furthermore, we observed an enhancement in the carrier mobility of DNA/1L-$MoS_2$, of almost one order of magnitude, attributed to the tensile strain. Our results demonstrate a diverse engineering possibility of bio-TMD hybrid structures for promising optoelectronic applications.

## 2. Experiment

First, the glass substrates ($22 \times 40 \times 1\,mm^3$) were cleaned with 1 M-KOH. Next, in order to obtain a charged and hydrophilic surface, the acetone and distilled water in ultrasonic bath were treated with piranha and RCA solution [26, 27]. The CVD-grown [28] 1L-$MoS_2$ was transferred onto these treated substrates using the wet transfer technique [29]. We eliminated the polymethyl methacrylate (PMMA) residues by continuously cleaning with acetone, IPA, and ethanol. This 1L-$MoS_2$ was subjected to oxygen plasma treatment using radio frequency (RF) plasma cell to obtain a hydrophilic 1L-$MoS_2$ surface. The oxygen plasma treatment was performed under an operating pressure of $1.3 \times 10^{-3}$ Pa, RF power of 50 W, and 5 sccm flow rate of oxygen gas for 5 s.

We purchased $\lambda$-DNA (0.3 $\mu$g/$\mu$L, Thermo Scientific Corp.) and YOYO-1 (1 mM solution in dimethyl sulfoxide, Invitrogen Corp.). For the fluorescence visualization of DNA stretching, we formed a YOYO-1 dye stained $\lambda$-DNA solution by mixing the exact amount of dye in the $\lambda$-DNA solution [30], and we centrifuged the mixture for 15 min under 3000 rpm at room temperature for effective intercalation. Finally, 50 $\mu$L of the DNA-dye solution was spin coated over the surface of the modified glass substrate containing plasma treated 1L-$MoS_2$ with a rotating speed of 4550 rpm for the first 20 s and 5750 rpm for an additional 10 s for optimal dispersion of stretched DNA [30].

For electrical measurements, 1L-$MoS_2$ was transferred onto the modified $SiO_2$/Si substrates using wet transfer techniques [29]. Using the normal photolithography technique, the source and drain electrodes of the devices were fabricated [31, 32]. For these electrodes, a 50 nm thick Au layer with Cr/5 nm was deposited by applying the electron beam evaporation technique [31, 32]. Moreover, the device was treated with oxygen plasma under the same conditions. DNA-YOYO-1 solution was spin coated over the device with similar experimental parameters, as described above. The electrical transport characteristics of the fabricated 1L-$MoS_2$ device with pristine state and after DNA stretching were tested in ambient conditions.

We used a lab-made inverted laser confocal microscope (LCM) system combined with a spectrometer for the measurements of confocal PL, Raman, and low temperature PL [12, 33]. Our samples were excited with a 514 nm wavelength line of an Ar-ion laser and a 633 nm wavelength line of a He-Ne laser for the Raman and PL measurements. We used an oil-immersion objective lens with a 1.4 numerical aperture for focusing the laser light on the samples and the same objective was used to collect the PL and Raman signals from the samples. The lateral resolution of the PL imaging and spectroscopy was estimated to be ~500 nm [34, 35]. The typical laser power values for the PL and Raman measurements were 70 $\mu$W and 300 $\mu$W, respectively. For exact comparison between pristine and DNA-stretched 1L-$MoS_2$, we used the same experimental parameters for each set of the PL and Raman measurements. The fluorescence images of DNA-stretched 1L-$MoS_2$ were taken with 436 nm line of Hg lamp. The FET measurements were performed using a four-probe station equipped with a current detector (Source Meter 2400, Keithley) at ambient condition.

## 3. Results and Discussion

While the deposition of DNA solution was previously used for DNA/TMD hybridization [23, 24], here we laterally stretched strands of DNA molecules on 1L-TMDs. Figure 1 shows the schematic for stretching the DNA molecules on the glass substrate and $MoS_2$ surface. Glass substrates treated with piranha and RCA solution, as described in the experimental section, developed negative charges on the surface [26, 27]. Subsequently, 1L-$MoS_2$ sample was transferred onto the modified substrate. Formation of hydrogen bonds between the alkyl functional group of YOYO-1 dye molecule and the amine functional group contained in the DNA molecule induced the intercalation of YOYO-1 molecules in the DNA [30]. To obtain a hydrophobic $MoS_2$ surface, we performed oxygen plasma treatment. We ensured that the oxygen plasma treatment did not affect the optical characteristics of 1L-$MoS_2$. (See Figure S1 in Supplementary Material available online at https://doi.org/10.1155/2017/2565703 for PL mapping images, PL spectra, and Raman spectra before and after oxygen plasma treatment.) Finally, YOYO-1 stained DNA molecules were spin coated. The two competitive forces of centrifugal force and the electrostatic force resulted in lateral stretching of the DNAs on the substrate and on the 1L-$MoS_2$ surface as well. In more detail, because YOYO-1 stained DNAs consist of positively charged amine groups and the substrate is negatively charged by piranha and RCA treatment, adhesive electrostatic force between the substrate and DNA molecules is developed. On the other hand, the spin coating process provides the centrifugal force applied to DNA strands and resulted in stretching of DNA molecules in specific orientation. The proper selection of spin coating

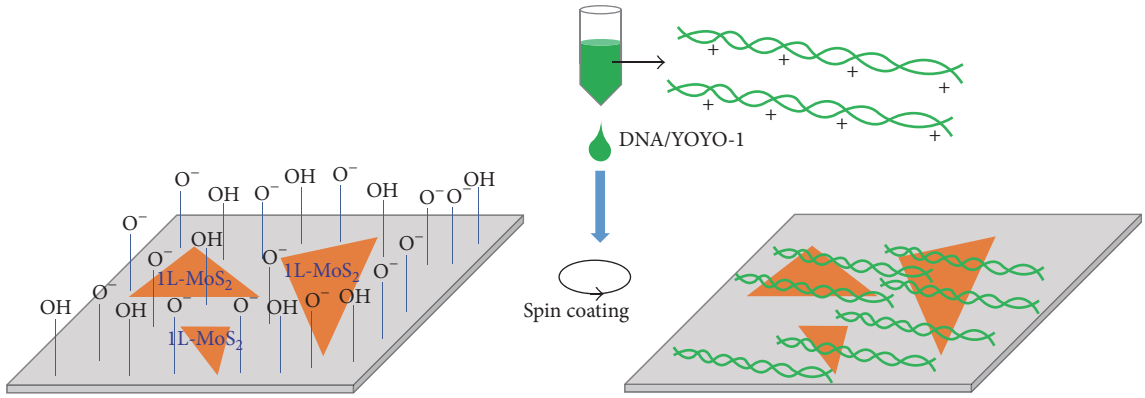


FIGURE 1: Schematic illustration of DNA stretching on 1L-$MoS_2$ surface. The surface of the glass substrate was negatively charged by piranha and RCA treatment (see the text) and YOYO-1 stained DNA strands were spin coated on the sample, which resulted in lateral stretching of DNA strands on 1L-$MoS_2$.

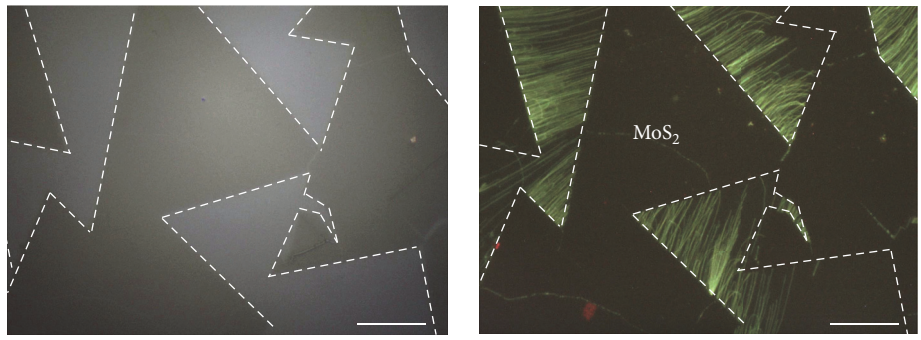


(a) (b)

FIGURE 2: (a) Bright-field optical image of the sample. (b) Epifluorescence image of YOYO-1-stained DNA strands stretched on 1L-$MoS_2$. 436 nm line of Hg lamp was used for fluorescence excitation. Scale bars indicate 10 $\mu$m.

parameters, such as rotating speed and time supports the good stretching of the DNA strands. Excessive spin speed can cause the shearing of DNA strands while low speed can cause the dispersion of coiled and aggregated DNA strand [30].

Figure 2 displays a bright-field microscope image and the fluorescence image of laterally stretched DNAs on CVD-grown 1L-$MoS_2$. The DNA strands were not visible in bright-field microscope image, owing to a significantly small diameter (~2 nm) of single DNA strands. However, the presence of strands of DNAs on the sample was clearly revealed in the fluorescence image by the fluorescence emitted from YOYO molecules incorporated in DNA chains, particularly between the triangular grains of CVD-grown 1L-$MoS_2$. Interestingly YOYO-1 fluorescence of DNAs is completely quenched in the region of $MoS_2$ grains. The absence of YOYO-1 fluorescence is likely to be caused by the charge transfer or the energy transfer from YOYO-1 to $MoS_2$.

We present the results of the PL spectra mappings of pristine 1L-$MoS_2$ and 1L-$MoS_2$ with laterally stretched DNAs using a 633 nm wavelength laser in Figures 3(a)–3(c). The representative PL intensity maps, PL spectra, and PL peak position maps are shown in Figures 3(a), 3(b), and 3(c), respectively. The laser light with a 633 nm wavelength is likely to be absorbed by 1L-$MoS_2$ and not by YOYO-1 dye, and therefore, the PL of 1L-$MoS_2$ can be studied without being interfered by the fluorescence of YOYO-1. The PL intensity of 1L-$MoS_2$ was found to be drastically reduced after the stretching of DNAs. The averaged PL spectra in Figure 3(b) display ~50% of reduction in the PL intensity of 1L-$MoS_2$ owing to the stretching of DNA molecules. The peak position maps of A excitons in Figure 3(c) show the significant red-shift of A exciton peak by ~16 nm in the DNA-stretched 1L-$MoS_2$. The red-shift of the PL peak has been interpreted as a result of an increase in the trion spectral weight originating from the increase of electron density [9, 12]. The reduction of PL intensity and red-shift of PL peak suggests the n-doping effect in 1L-$MoS_2$ after the lateral stretching of DNAs on 1L-$MoS_2$. We did not observe any noticeable defect passivation or increase in 1L-$MoS_2$ caused by DNA stretching in low temperate PL spectra as shown in Figure 3(d), which suggests that the likely change of defect states of 1L-$MoS_2$ after the DNA stretching is not responsible for the observed modification of PL spectra.

The averaged Raman spectra in Figure 3(e) show the red-shift on both the $E^1{}_{2g}$ and $A_{1g}$ Raman modes in 1L-$MoS_2$ by 5 and 3 $cm^{-1}$, respectively, after DNA stretching. The red-shift

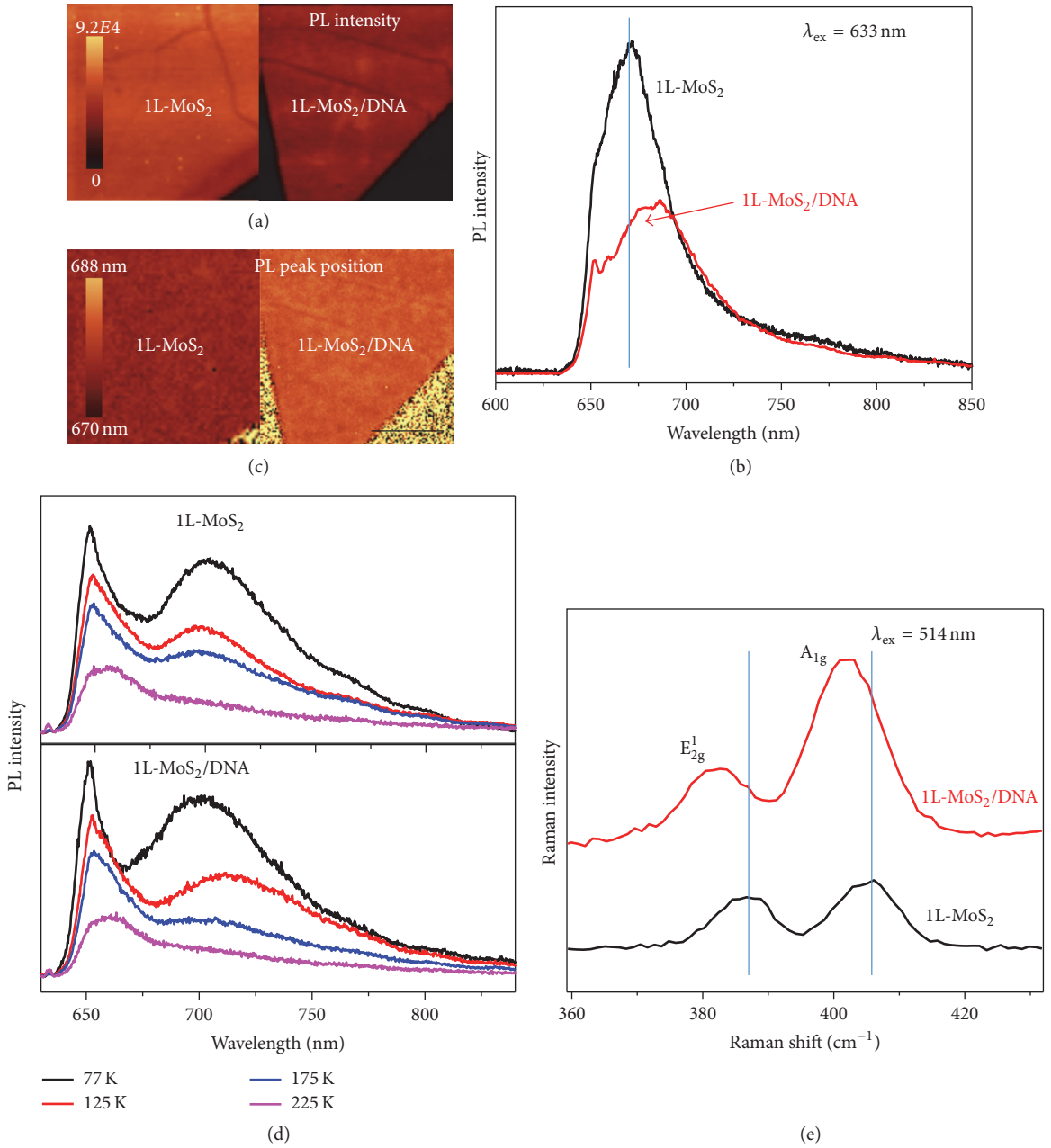


FIGURE 3: (a) PL intensity maps of pristine and DNA-stretched 1L-$MoS_2$ with the laser excitation of 633 nm line. (b) Averaged PL spectra, (c) peak position maps of A exciton peaks, (d) temperature-dependent PL spectra, and (e) averaged Raman spectra obtained from pristine 1L-$MoS_2$ and DNA-stretched 1L-$MoS_2$. Scale bars indicate 5 $\mu$m.

of the $E^1_{2g}$ mode for DNA/$MoS_2$ systems was previously observed [23, 24] and the observed red-shift in the peak position of the $E^1_{2g}$ Raman mode indicates the presence of tensile strain in 1L-$MoS_2$ with lateral stretching of DNAs, which amount to ~1% according to previous empirical results [10, 36]. The red-shift of A exciton PL peak and $A_{1g}$ Raman mode in DNA-stretched 1L-$MoS_2$ can be caused by electron doping in 1L-$MoS_2$ [9, 12]. The $A_{1g}$ Raman mode shift of 3 $cm^{-1}$ corresponds to an increase of ~1.4 × $10^{13}$/$cm^2$ in the electron density [37]. The presence of a negatively charged phosphate group in the backbone of the DNA may be the origin of such electron doping effect [24, 25]. In addition, the tensile strain may be responsible for the observed red-shift of PL peak energy in our DNA/1L-$MoS_2$, since tensile strain is known to reduce the bandgap of 1L-$MoS_2$ [10, 36] and thus we expect stretched DNA molecules could cause the band gap modulation of 1L-$MoS_2$. Unfortunately, we cannot precisely separate the effects of doping and strain because observed PL peak shift is the result of both effects. However, as the $A_{1g}$ mode and $E^1_{2g}$ mode are known to represent the strain and

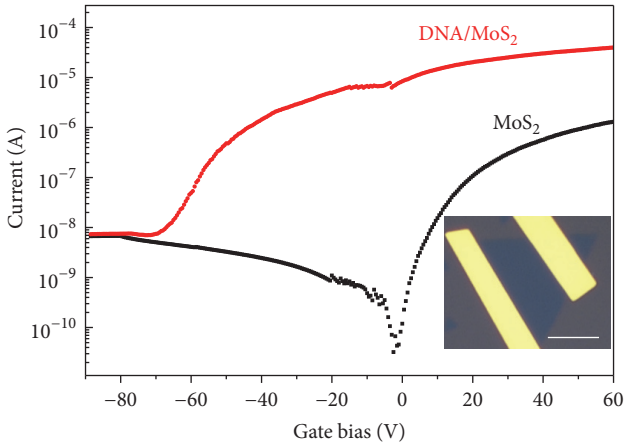


FIGURE 4: FET transport characteristics of pristine 1L-$MoS_2$ and DNA-stretched 1L-$MoS_2$. Inset shows the optical image of the FET device. Scale bar indicates 20 $\mu$m.

the electron density of 1L-$MoS_2$ independently, our results suggest the coexistence of electron doping effect and tensile strain in 1L-$MoS_2$ owing to the stretching of DNA strands.

We found that modulation of PL and Raman spectra was dependent upon the density of DNAs stretched on 1L-$MoS_2$, being less if a less number of DNAs were stretched. As displayed in Figure S2, we observed ~11 nm of red-shift and ~40% reduction in PL intensity of A exciton PL peak and 2.8 and 4.0 $cm^{-1}$ of $A_{1g}$ and $E^1{}_{2g}$ Raman peaks from the region with seemingly less density of stretched DNAs than in the region shown in Figure 2. This result suggests some degree of tunability of optical properties of DNA/1L-$MoS_2$ hybrid by controlling the density of stretched DNA molecules.

We studied the effect of DNA stretching on the electrical transport of 1L-$MoS_2$ using a back-gated FET configuration. Figure 4 shows the plot of source-drain current versus gate bias ($I_{ds}$–$V_g$) with a source-drain voltage of 1 V for pristine 1L-$MoS_2$, after the stretching of DNA strands. First, we note that the threshold voltage shifted by −68 V as a result of the DNA stretching. Moreover, we extracted the field-effect electron mobility ($\mu_{FE}$) values from the transport curves according to the equation $\mu_{FE} = dI_{ds}/dV_{ds}(L/WC_iV_{ds})$, where $C_i$ is the capacitance between the $MoS_2$ channel and the silicon layer per unit area and $L$ and $W$ are the length and width of the channel, respectively [32]. $\mu_{FE}$ values of 2.5 and 22.4 $cm^2\,V^{-1}\,s^{-1}$ were estimated for the pristine state of 1L-$MoS_2$ and for our DNA/1L-$MoS_2$ device, respectively, indicating a significant enhancement in the electron mobility on 1L-$MoS_2$ as a result of laterally stretched DNA strands. The electron mobility can be enhanced by reducing the structural defects or enhancing the carrier density of 1L-$MoS_2$ [38, 39]. Furthermore, theoretical studies have predicted that introducing tensile strain to 1L-$MoS_2$ can increase the field-effect mobility owing to a decrease in the effective mass of the electrons [15, 18]. Considering that a low temperature PL shows limited difference in terms of defect-oriented emission (Figure 3(e)), we believe that there exists no significant reduction in defect density with DNA stretching. We noticed the slight decrease of on-off current ratio in the DNA/1L-$MoS_2$ FET, which was in the order of $10^4$ in the hybrid structure while it was in the order of $10^5$ in the pristine state. The observed decrease of on-off ration could originate from the reduction of bandgap [40] that may have occurred by the introduction of tensile strain by DNA stretching.

## 4. Conclusion

We prepared a bio-TMD nanostructure by laterally stretching the DNAs on 1L-$MoS_2$. We observed a strong modification of photoluminescence and Raman spectra with reduced PL intensity and red-shift of the PL peak and Raman peaks in 1L-$MoS_2$, which were attributed to electron doping by the DNAs and the presence of tensile strain in 1L-$MoS_2$. We also observed a significant enhancement of electric mobility in DNA/1L-$MoS_2$ heterostructure compared to that in pristine 1L-$MoS_2$, which is likely to be caused by the induced strain in 1L-$MoS_2$. The optical characteristics of the stretched DNAs on 1L-$MoS_2$ were also strongly modified, originating from the effects of charge transfer and tensile strain. The carrier mobility of 1L-$MoS_2$ has significantly increased with stretched DNAs on 1L-$MoS_2$, suggesting promising optoelectronic application of bio-TMD hybrid nanostructures.

## Conflicts of Interest

The authors declare that there are no conflicts of interest regarding the publication of this paper.

## Acknowledgments

This work was supported by IBS-R011-D1.

## References

[1] K. F. Mak, C. Lee, J. Hone, J. Shan, and T. F. Heinz, "Atomically thin MoS2: a new direct-gap semiconductor," *Physical Review Letters*, vol. 105, no. 13, Article ID 136805, 2010.

[2] B. Radisavljevic, A. Radenovic, J. Brivio, V. Giacometti, and A. Kis, "Single-layer $MoS_2$ transistors," *Nature Nanotechnology*, vol. 6, no. 3, pp. 147–150, 2011.

[3] K. F. Mak, K. He, C. Lee et al., "Tightly bound trions in monolayer $MoS_2$," *Nature Materials*, vol. 12, no. 3, pp. 207–211, 2013.

[4] G. P. Neupane, K. P. Dhakal, H. Kim et al., "Formation of nano-sized monolayer $MoS_2$ by oxygen-assisted thinning of multilayer $MoS_2$," *Journal of Applied Physics*, vol. 120, no. 5, Article ID 051702, 2016.

[5] J. S. Ross, S. Wu, H. Yu et al., "Electrical control of neutral and charged excitons in a monolayer semiconductor," *Nature Communications*, vol. 4, article 1474, 2013.

[6] D. O. Sigle, J. Mertens, L. O. Herrmann et al., "Monitoring morphological changes in 2D monolayer semiconductors using atom-thick plasmonic nanocavities," *ACS Nano*, vol. 9, no. 1, pp. 825–830, 2015.

[7] K. C. J. Lee, Y.-H. Chen, H.-Y. Lin et al., "Plasmonic gold nanorods coverage influence on enhancement of the photoluminescence of two-dimensional $MoS_2$ monolayer," *Scientific Reports*, vol. 5, Article ID 16374, 2015.

[8] H.-Y. Park, M.-H. Lim, J. Jeon et al., "Wide-range controllable n-doping of molybdenum disulfide ($MoS_2$) through thermal and optical activation," *ACS Nano*, vol. 9, no. 3, pp. 2368–2376, 2015.

[9] S. Mouri, Y. Miyauchi, and K. Matsuda, "Tunable photoluminescence of monolayer $MoS_2$ via chemical doping," *Nano Letters*, vol. 13, no. 12, pp. 5944–5948, 2013.

[10] H. J. Conley, B. Wang, J. I. Ziegler, R. F. Haglund Jr., S. T. Pantelides, and K. I. Bolotin, "Bandgap engineering of strained monolayer and bilayer $MoS_2$," *Nano Letters*, vol. 13, no. 8, pp. 3626–3630, 2013.

[11] Y. Wang, C. Cong, W. Yang et al., "Strain-induced direct–indirect bandgap transition and phonon modulation in monolayer $WS_2$," *Nano Research*, vol. 8, no. 8, pp. 2562–2572, 2015.

[12] K. P. Dhakal, D. L. Duong, J. Lee et al., "Confocal absorption spectral imaging of $MoS_2$: optical transitions depending on the atomic thickness of intrinsic and chemically doped $MoS_2$," *Nanoscale*, vol. 6, no. 21, pp. 13028–13035, 2014.

[13] D. Sun, Y. Rao, G. A. Reider et al., "Observation of rapid exciton-exciton annihilation in monolayer molybdenum disulfide," *Nano Letters*, vol. 14, no. 10, pp. 5625–5629, 2014.

[14] E. Scalise, M. Houssa, G. Pourtois, V. Afanas'ev, and A. Stesmans, "Strain-induced semiconductor to metal transition in the two-dimensional honeycomb structure of $MoS_2$," *Nano Research*, vol. 5, no. 1, pp. 43–48, 2012.

[15] H. Shi, H. Pan, Y.-W. Zhang, and B. I. Yakobson, "Quasiparticle band structures and optical properties of strained monolayer $MoS_2$ and $WS_2$," *Physical Review B*, vol. 87, no. 15, Article ID 155304, 2013.

[16] H. Pan and Y.-W. Zhang, "Tuning the electronic and magnetic properties of $MoS_2$ nanoribbons by strain engineering," *Journal of Physical Chemistry C*, vol. 116, no. 21, pp. 11752–11757, 2012.

[17] P. Lu, X. Wu, W. Guo, and X. C. Zeng, "Strain-dependent electronic and magnetic properties of $MoS_2$ monolayer, bilayer, nanoribbons and nanotubes," *Physical Chemistry Chemical Physics*, vol. 14, no. 37, pp. 13035–13040, 2012.

[18] M. Hosseini, M. Elahi, M. Pourfath, and D. Esseni, "Strain induced mobility modulation in single-layer $MoS_2$," *Journal of Physics D: Applied Physics*, vol. 48, no. 37, Article ID 375104, 2015.

[19] X. Li, J. Zhu, and B. Wei, "Hybrid nanostructures of metal/two-dimensional nanomaterials for plasmon-enhanced applications," *Chemical Society Reviews*, vol. 45, no. 11, pp. 3145–3187, 2016.

[20] Z. Luo, J. Zhou, L. Wang, G. Fang, A. Pan, and S. Liang, "Two-dimensional hybrid nanosheets of few layered $MoSe_2$ on reduced graphene oxide as anodes for long-cycle-life lithium-ion batteries," *Journal of Material Chemistry A*, vol. 4, no. 40, pp. 15302–15308, 2016.

[21] E. H. Cho, W. G. Song, C. J. Park, J. Kim, S. Kim, and J. Joo, "Enhancement of photoresponsive electrical characteristics of multilayer $MoS_2$ transistors using rubrene patches," *Nano Research*, vol. 8, no. 3, pp. 790–800, 2015.

[22] S. H. Yu, Y. Lee, S. K. Jang et al., "Dye-sensitized $MoS_2$ photodetector with enhanced spectral photoresponse," *ACS Nano*, vol. 8, no. 8, pp. 8285–8291, 2014.

[23] H.-Y. Park, S. R. Dugasani, D.-H. Kang et al., "M-DNA/transition metal dichalcogenide hybrid structure-based bio-FET sensor with ultra-high sensitivity," *Scientific Reports*, vol. 6, no. 1, Article ID 35733, 2016.

[24] H.-Y. Park, S. R. Dugasani, D.-H. Kang et al., "n- and p-Type doping phenomenon by artificial DNA and M-DNA on two-dimensional transition metal dichalcogenides," *ACS Nano*, vol. 8, no. 11, pp. 11603–11613, 2014.

[25] D.-H. Kang, S. R. Dugasani, H.-Y. Park et al., "Ultra-low doping on two-dimensional transition metal dichalcogenides using DNA nanostructure doped by a combination of lanthanide and metal ions," *Scientific Reports*, vol. 6, Article ID 20333, 2016.

[26] T. M. McIntire, S. R. Smalley, J. T. Newberg, A. S. Lea, J. C. Hemminger, and B. J. Finlayson-Pitts, "Substrate changes associated with the chemistry of self-assembled monolayers on silicon," *Langmuir*, vol. 22, no. 13, pp. 5617–5624, 2006.

[27] H.-W. Liu, W.-K. Lai, S.-Y. Yu, S. C. Huang, and H.-C. Cheng, "Effects of RCA clean-up procedures on the formation of roughened poly-Si electrodes for high-density DRAMs' capacitors," *Materials Chemistry and Physics*, vol. 51, no. 2, pp. 195–198, 1997.

[28] G. H. Han, N. J. Kybert, C. H. Naylor et al., "Seeded growth of highly crystalline molybdenum disulphide monolayers at controlled locations," *Nature Communication*, vol. 4, article 1474, 2013.

[29] Y. Gong, Z. Lin, G. Ye et al., "Tellurium-assisted low-temperature synthesis of $MoS_2$ and $WS_2$ monolayers," *ACS Nano*, vol. 9, no. 12, pp. 11658–11666, 2015.

[30] G. P. Neupane, K. P. Dhakal, M. S. Kim et al., "Simple method of DNA stretching on glass substrate for fluorescence imaging and spectroscopy," *Journal of Biomedical Optics*, vol. 19, no. 5, Article ID 051210, 2014.

[31] K. Cho, M. Min, T.-Y. Kim et al., "Electrical and optical characterization of $MoS_2$ with sulfur vacancy passivation by treatment with alkanethiol molecules," *ACS Nano*, vol. 9, no. 8, pp. 8044–8053, 2015.

[32] M. Amani, D.-H. Lien, D. Kiriya et al., "Near-unity photoluminescence quantum yield in $MoS_2$," *Science*, vol. 350, no. 6264, pp. 1065–1068, 2015.

[33] G. P. Neupane, K. P. Dhakal, E. H. Cho et al., "Enhanced luminescence and photocurrent of organic microrod/ZnO nanoparticle hybrid system: nanoscale optical and electrical characteristics," *Electronic Materials Letters*, vol. 11, no. 5, pp. 741–748, 2015.

[34] S. Park, M. S. Kim, H. Kim et al., "Spectroscopic visualization of grain boundaries of monolayer molybdenum disulfide by stacking bilayers," *ACS Nano*, vol. 9, no. 11, pp. 11042–11048, 2015.

[35] Y. Lee, S. Park, H. Kim, G. H. Han, Y. H. Lee, and J. Kim, "Characterization of the structural defects in CVD-grown monolayered $MoS_2$ using near-field photoluminescence imaging," *Nanoscale*, vol. 7, no. 28, pp. 11909–11914, 2015.

[36] Y. Wang, C. Cong, C. Qiu, and T. Yu, "Raman spectroscopy study of lattice vibration and crystallographic orientation of monolayer $MoS_2$ under uniaxial strain," *Small*, vol. 9, no. 17, pp. 2857–2861, 2013.

[37] B. Chakraborty, A. Bera, D. V. S. Muthu, S. Bhowmick, U. V. Waghmare, and A. K. Sood, "Symmetry-dependent phonon renormalization in monolayer $MoS_2$ transistor," *Physical Review B*, vol. 85, no. 16, Article ID 161403, 2012.

[38] J. Hong, Z. Hu, M. Probert et al., "Exploring atomic defects in molybdenum disulphide monolayers," *Nature Communications*, vol. 6, article 6293, 2015.

[39] S. Andleeb, A. K. Singh, and J. Eom, "Chemical doping of $MoS_2$ multilayer by p-toluene sulfonic acid," *Science and Technology of Advanced Materials*, vol. 16, no. 3, Article ID 035009, 2015.

[40] N. Harada, S. Sato, and N. Yokoyama, "Computational study on electrical properties of transition metal dichalcogenide field-effect transistors with strained channel," *Journal of Applied Physics*, vol. 115, no. 3, Article ID 034505, 2014.